Journal of Petroleum Science and Technology 15(1): 45, 2025, Pages 60-71
DOI:10.22078/jpst.2026.5725.1980

Journal of Petroleum Science and Technology
Research Paper
https://jpst.ripi.ir/

Providing the New Energy-Exergy-Water Nexus-Based Strategy for a Petrochemical Unit

Azadeh Shahidian*[1], Milad Davoudian[1] and Mohammad Reza Habibi[2]
1. Department of Mechanical Engineering K. N. Toosi University of Technology, Tehran, Iran
2. Energy Technologies Research Division, Research Institute of Petroleum Industry (RIPI), Tehran, Iran

Abstract
Population growth and industrial development have led to rising electricity demand, greenhouse gas emissions, and water consumption. On the other hand, climate change can influence the amount of available renewable water. In this article, part of the steam cycle of Petrochemical Unit A has been modeled, analyzed, and reviewed. Scenarios and suggestions for saving steam and energy have also been presented, and the savings for these scenarios have been calculated economically, considering the rates of the desired utilities. For this purpose, the Engineering Equation Solver (EES) software is used. Moreover, a mass balance analysis of the proposed steam cycle is first conducted, followed by the calculation of key performance parameters, including efficiency, exergy, and power, for the various equipment units. Finally, different solutions and scenarios are evaluated to assess opportunities for water and energy optimization in the steam cycle of Petrochemical Unit A. By implementing scenarios for a condensing steam turbine, the STC-3001, steam consumption is reduced by 1.5 to 10.7 tons/hour, equivalent to annual savings of $210,000 to $1,433,507, depending on the intended utilities. Furthermore, by improving the steam system of the STC-1001 gland turbine, the amount of its steam consumption is reduced by about 6 tons/hour, equivalent to an annual savings of $778,400.

Keywords: Water-Energy Nexus, Steam Cycle, Steam Producer and Consumer, Improving Water and Energy Consumption, Petrochemical Unit.

Introduction
Water and energy resources are inseparably intertwined and interdependent because large amounts of energy are needed for water pumping, filtering, transferring, heating, cooling, and recycling, while water is used for power generation as steam to rotate turbine blades and primary coolant in thermal power plants [1]. Over the past decade, the water–energy nexus has received growing attention from both the scientific and policy communities. The rapid growth of urbanization and population, together with global economic development, places significant pressure on Earth's limited resources, including water, energy, food, land, and ecosystems. Consequently, water and energy conservation has become a key prerequisite for sustainable development worldwide [2]. Moreover, industrial water consumption accounts for a considerable share of global annual water withdrawal, representing 19% of the total [3]. Furthermore, global warming and climate change have exacerbated water scarcity, causing it to reach critical levels in many regions. Based on estimates, 34 countries experience water stress at approximately 25%-75%, while 25 countries, including Iran, have water stress above 75% [4]. Moreover, O. R. Altarawneh et al. conducted an energy and exergy assessment of a combined heat and power (CHP) plant in Jordan to identify the components responsible for the highest energy losses due to irreversibilities. The study further sought to enhance the plant's performance by locating major sources of energy loss and proposing corrective measures to reduce them [5]. In addition, M.H. Hamayun et al. studied a steam power plant based on energy and exergy analysis. Moreover, their analysis indicated that the boiler is the primary source of exergy destruction due to the incomplete combustion process and inadequate insulation. Additionally, the exergy efficiency (%) and the exergy destruction rate (kW) of the power plant equipment were calculated [6]. A. G. Celik et al. investigated a 210 MW coal-fired thermal power plant in Turkey using real operating data collected under different ambient temperature conditions. The

**Corresponding author:* Azadeh Shahidian, *Department of Mechanical Engineering K. N. Toosi University of Technology, Tehran, Iran*
E-mail addresses: shahidian@kntu.ac.ir
Received 2025-07, Received in revised form 2026-05-20, Accepted 2026-04-22, Available online .....

authors performed an exergy analysis and an exergy-based sustainability assessment. The results of the exergy analysis indicated that 59.01% of the total exergy destruction occurred in the boiler, while 29.12% was attributed to the intermediate-pressure turbine. The findings of the study provide useful insights for investors and researchers in making more informed decisions regarding the design of future thermal power plants [7].

M. Tontu et al. performed a comparative study of subcritical, supercritical, and ultra-supercritical steam power plants. Energy and exergy analyses were employed to evaluate the thermodynamic performance of each plant and its major equipment. The results indicated that the ultra-supercritical configuration achieved the highest energy and exergy efficiencies, primarily due to reduced coal consumption. The energy efficiencies of the subcritical, supercritical, and ultra-supercritical plants were reported as 41.5%, 43.8%, and 46.0%, respectively, while the corresponding exergy efficiencies were 39.1%, 40.8%, and 41.9%, respectively [8].

M. Mohseni et al. investigated the optimization of power generation in a thermal power plant in Iran through the replacement of the existing boiler with a heat recovery steam generator (HRSG). A comprehensive analysis of the existing steam cycle revealed that the boiler, turbine, and condenser were responsible for the highest rates of exergy destruction. The study also showed that the six heaters and the boiler supplied 25% and 70% of the turbine inlet energy, respectively. Furthermore, the analysis of the combined cycle indicated that the first-law and second-law efficiencies increased by 27% and 26%, respectively.

U. G. Azubuike et al. investigated the exergy performance of a 200 MW gas-fired steam turbine power plant under both full-load and part-load operating conditions. The results showed that the boiler exhibited the lowest exergy efficiencies among all major components, with values of 42.8%, 42.5%, and 41.8% at 100% 75%, and 50% load, respectively. At 25% load, the condenser recorded the lowest exergy efficiency of 40.29%. The study also presented a ranking of the power plant components based on their exergy performance [10].

M. Galal et al. studied the exergy and energy analysis of a steam cycle in a sulfuric acid unit. In this study, a mathematical model was developed using EES software to perform the calculations. Furthermore, the study identified the boilers as the primary sources of exergy destruction, followed by the heaters, steam turbines, and condensers. It also examined the effects of various operating parameters, including ambient temperature, on the performance of the unit's major components. Moreover, the influence of steam inlet temperature, pressure, and mass flow rate on the overall exergetic efficiency of the unit was assessed. [11]. Moreover, M. E. Walker et al. investigated and estimated water consumption and steam production in the manufacturing industries of the United States. In addition, the authors estimated the amount of freshwater consumed in industrial steam systems in the United States. The estimates were obtained using a thermodynamic steam system model based on fuel consumption and industry-specific operating characteristics. These estimates were divided by the steam/water demand source in each sub-section, including direct injection into processes, boiler blowdown, valve losses, and system leakage and failure [12]. Hu et al. developed a thermodynamic model of a 660 MW thermal power plant incorporating a hybrid cooling system (HCS) and analyzed the influence of dry-bulb temperature and relative humidity on its thermodynamic performance using the Epsilon calculation code. The performance of the HCS was subsequently evaluated and compared with that of dry cooling systems (DCS) and wet cooling systems (WCS) [13]. W. Asvapoostikul et al. investigated the performance of a hybrid cooling system (HCS) using both experimental testing and numerical simulations under a wide range of operating conditions [14]. A computational model was developed to predict the performance of dry cooling systems (DCS), wet cooling systems (WCS), and HCSs. G. Ahmadi et al. performed an energy, exergy, and environmental (3E) assessment of a combined heat and power (CHP) system in a petrochemical facility. The system consisted of steam generators, turbogenerators, and a steam distribution network serving process consumers. Their findings revealed that the boilers, steam pressure-reducing stations, and turbogenerators were the major sources of exergy destruction, respectively [15]. Moreover, G. R. Ahmadi et al. performed energy and exergy analyses of the Shahid Montazeri Steam Power Plant in Iran. The thermodynamic performance of the plant components was evaluated under various operating conditions, and potential approaches for enhancing the overall efficiency of the power plant were identified [16]. B. Ali analyzed future water demand patterns in the energy sector and identified high-demand development trajectories. The study also evaluated water requirements associated with primary fuel production and electricity generation in Alberta, Canada [17]. Furthermore, A. M. K. Vandani et al. investigated boiler blowdown heat recovery in steam power plants through energy and exergy analyses. A steam power plant in Iran was selected as a case study to evaluate the effects of implementing a heat recovery system on overall plant performance [18]. Moreover, A. Gu et al. quantitatively investigated the energy–water nexus in China and evaluated the effects of energy conservation policies on water consumption in selected industrial sectors, including ferrous and non-ferrous metals, petrochemicals, and building materials, during China's 11th Five-Year Plan [19]. O. J. Khaleel et al. conducted a comprehensive review of thermal power plants, with particular emphasis on cycle configurations, modeling approaches, simulation techniques, and performance enhancement strategies. The review examined energy and exergy analyses as well as exergy destruction assessments for major plant components and summarized various methods for improving thermal power plant performance [20].

In view of the growing importance of water conservation in the petrochemical industry, particularly in urea and ammonia production plants, this study focuses on the modeling, analysis, and evaluation of a section of the steam cycle in Petrochemical Unit A. This study was motivated by the limited availability of comprehensive research on the steam cycle of urea and ammonia production units. To achieve the objectives of the study, the system was divided into 51 state points, and the thermodynamic properties and performance indicators were determined using Engineering Equation Solver (EES) software based on the mass flow rate, temperature, and pressure data at each point The calculated indicators

included power output, thermal efficiency, exergy efficiency, exergy destruction rate, and mass balance. In addition, several energy- and steam-saving scenarios were proposed and economically evaluated using the corresponding utility costs. Where necessary, simulations were performed using the Thermoflex module of Thermoflow software. Finally, water-saving strategies for selected petrochemical equipment were assessed, and the associated economic savings were quantified on hourly, daily, and annual bases.

Materials and Methods

Problem Statement

This study focuses on the modeling and analysis of a section of the steam cycle in the third phase of ammonia and urea production at Petrochemical Company A. The required thermodynamic and performance parameters are determined using Engineering Equation Solver (EES) software The modeled steam cycle comprises condensing and back-pressure steam turbines, very-high-pressure (VHP), high-pressure (HP), and low-pressure (LP) steam headers, shell-and-tube condensers, boilers feedwater pumps, deaerators, steam drums, and pressure-reducing valves (Fig. 1). The energy, exergy, and mass balance equations governing the aforementioned equipment are solved using Engineering Equation Solver (EES) software, enabling the evaluation of key performance parameters including power output and efficiency.

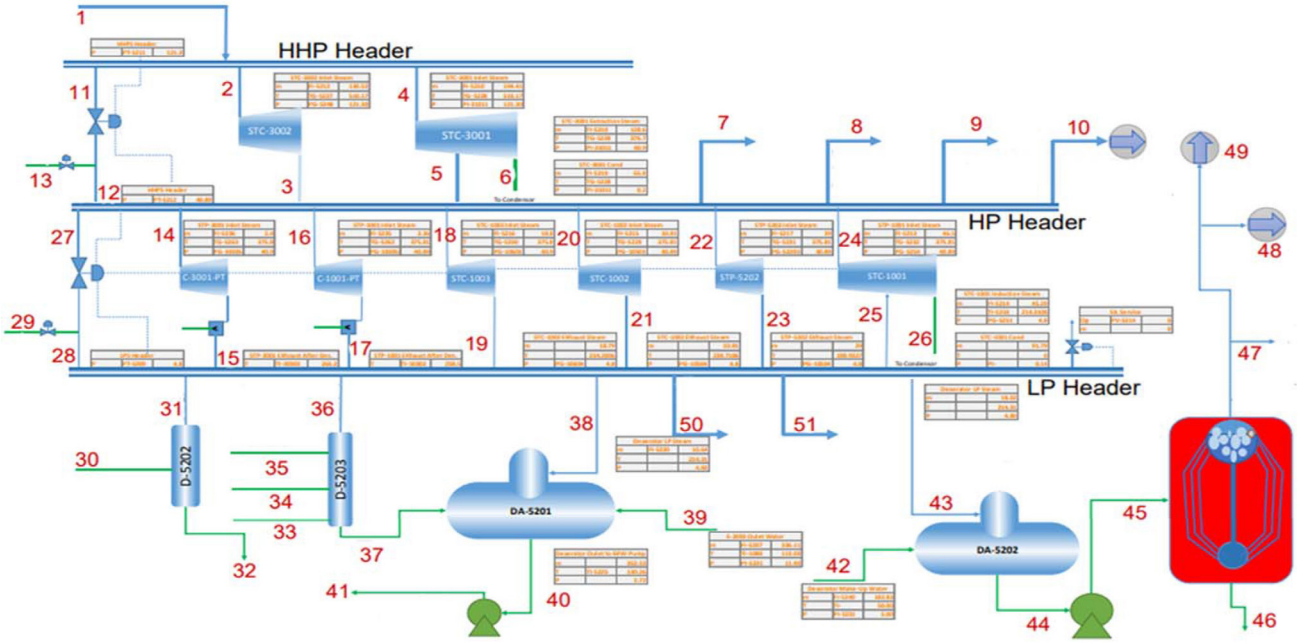

Fig. 1 Petrochemical unit steam system.

In the analyzed system, the steam supplied to the high-pressure (HP) header (Point 1) originates from the SB-5201 boiler. The SB-5202 boiler provides steam to another production phase within the petrochemical complex. For thermodynamic analysis, the system is divided into 51 state points. The temperature (°C) pressure (bar), and mass flow rate (t/h) at each point are used as input data for calculating key performance indicators, including steam-header mass balances, power generation, energy efficiency, exergy efficiency and exergy destruction rates of the various system components. Table 1 provides the characteristics of each point of the flow.

The main limitations of this study are presented below before introducing the governing equations and the subsequent sections of the paper:

1) The low prices of energy carriers and water in countries where these resources are heavily subsidized reduce the economic incentive to invest in water and energy conservation projects.

2) Ensuring product quality and process stability: Changes in operating conditions, including temperature, pressure, and steam flow rate, intended to reduce water consumption may adversely affect product quality and process stability. As a result, petrochemical companies generally prioritize maintaining production targets and product quality, while water and energy conservation initiatives receive comparatively less attention.

3) The need to stop the unit for optimization; To implement these scenarios for reducing water and energy consumption, some of the equipment of the industrial unit may need to be temporarily taken out of operation. Therefore, the company will incur financial losses. These scenarios can be implemented during scheduled maintenance shutdowns or turnarounds that are typically conducted every few years.

Governing Equations

The system under study was modeled using a set of governing equations and correlations, as follows.

In this section, the exergy relations are calculated with respect to the ambient pressure and temperature. In the exergy analysis, the conservation laws of mass and energy are applied. The pump and turbine are modeled based on isentropic efficiency under steady-state operating conditions. The working fluid is assumed to be incompressible in the pump and compressible in the turbine.

Tabel 1 Characteristics of flows in the evaluated system [21].

Stream Number	Mass Flow Rate	Temperature	Pressure (bar)
1	341.6845	510.17	121.3
2	130.52	510.17	121.3
3	130.52	375.1	40.89
4	194.41	510.17	121.3
5	128.6	376.7	40.89
6	65.8	53	0.2
7	154.3	375.8097	40.89
8	5.91	375.8097	40.89
9	2.7	375.8097	40.89
10	0.667088	375.8097	40.89
11	16.4565	510.17	121.3
12	16.4565	375.1	40.89
13	0	0	0
14	2.4	375.8	40.89
15	2.4	265.2	4.8
16	2.26	375.8	40.89
17	2.26	258.5	4.8
18	18.8	375.8	40.89
19	18.8	234.2006	4.8
20	10.81	375.8	40.89
21	10.81	238.7186	4.8
22	29	375.8	40.89
23	29	188.9327	4.8
24	46.5	375.8	40.89
25	45.29	214.3108	408
26	91.97	53	0.14
27	2.229462	375.8	40.89
28	2.229462	265	4.8
29	6.904928	250	4.8
30	3.6	326.8293	4.8
31	1.49	150.3	4.8
32	2.11	150.3	4.8
33	2.7	254	4.8
34	1.157	328	4.8
35	5.673	328	4.8
36	3.40563	150.3045	4.8
37	6.12	150.3	4.8
38	10.64	214.31	4.8
39	336.11	113	11.9
40	352.53	130.26	2.72
41	341.3865	130	121.3
42	182.83	50	4.8
43	18.02	214.31	4.8
44	317.1	107	2.29
45	158.55	107	58
46	0.99885	257.4394	45
47	5.87	390	45
48	18	390	45
49	175.9	390	45
50	2.35	214.3108	4.8
51	1	214.3108	4.8

Furthermore, frictional losses between the fluid and the components are neglected.
The physical exergy of flows is obtained from the following equation (Equation 1) [22, 23]:

$$\psi = \dot{m}\left[(h_i - h_o) - T_0 \times (s_i - s_o)\right] \quad (1)$$

Exergy destruction rate is in the form of the following relationship (Equation 2):

$$I = \left| Ex_{in} - Ex_{out} \right| \quad (2)$$

Ex_{in} and Ex_{out} are input exergy and output exergy, respectively. The isentropic efficiency of the turbine and the turbine power output are defined by Equations (3) and (4) respectively.

$$\eta_{th,Tyrbine} = \frac{W_a}{W_s} = \frac{h1 - h2a}{h1 - h2s} \quad (3)$$

$$\dot{W} = \dot{m} \times (h_1 - h_{2a}) \quad (4)$$

he isentropic efficiency and power of the pumps are calculated in the form of relations (5) and (6):

$$\eta_{th,pump} = \frac{W_s}{W_a} = \frac{v(p_2 - p_1)}{h_{2a} - h_1} = \frac{h_{2s} - h_1}{h_{2a} - h_1} \quad (5)$$

$$\dot{W}_{pump} = \dot{m} \times (h_2 - h_1) \quad (6)$$

The exergy efficiency of pumps and turbines is as follows:

$$\eta_{exergy} = \frac{Ex_{out}}{Ex_{in}} \quad (7)$$

In condensers, exergy efficiency and exergy destruction rate are calculated in the form of relations (8) and (9):

$$\eta_{exergy} = \frac{\dot{m}_c (\psi_e - \psi_i)_c}{\dot{m}_h (\psi_i - \psi_e)_h} \quad (8)$$

$$I = Ex_{cold,in} - Ex_{cold,out} \quad (9)$$

In the above equations, subscript c refers to the cold stream and subscript h refers to the hot stream. The exergy efficiency and exergy destruction rate of the deaerators and steam drums are evaluated using the following relations (Equations 10 and 11):

$$\eta_{exergy} = \frac{\Sigma Ex_{outlet}}{\Sigma Ex_{inlet}} \quad (10)$$

$$I = \left| \sum Ex_{inlet} - \sum Ex_{outlet} \right| \quad (11)$$

The exergy efficiency and exergy destruction rate of the boilers are evaluated using the following relations (Equations 12 and 13):

$$\eta_{exergy} = \frac{Ex_{in} - Ex_{out}}{Ex_{fuel}} \quad (12)$$

$$I = Ex_{fuel} + Ex_{in} - Ex_{out} \quad (13)$$

Ex_{fuel}, is chemical exergy of the fuel. The fuel used in this cycle is natural gas (CH_4). Also, the chemical exergy of the fuel is calculated as follows (Equations 14 and 15):

$$Ex_{chemical,fuel} = \gamma_f \times \dot{m}_f \times LHV \quad (14)$$

$$Ex_{fuel,total} = Ex_{fuel,boiler1} + Ex_{fuel,boiler2} \quad (15)$$

The low heating value (LHV) of the fuel for natural gas is 47.3 megajoules and the exergy factor (γ_f) for it is 1.03 [5]. Also, $\dot{m}_f$ expresses the fuel mass flow rate. The fuel flow rate of the main boiler (SB-5201) whose produced steam enters the HHP steam header at point 1 of the cycle is equal to 55 tons/hour and the fuel flow rate of the side boiler of the cycle is equal to 14.7 tons/hour.

$$\eta_{exergy,cycle} = \frac{\dot{W}_{net,cycle}}{Ex_{fuel,boiler1} + Ex_{fuel,boiler2}} \times 100 \quad (16)$$

$$\dot{W}_{net,cycle} = \Sigma \dot{W}_T - \Sigma \dot{W}_P \quad (17)$$

Using the results obtained from Equations 16 and 17, the exergy efficiency of the whole system is 45.64% and the net power of the system is 48866 kw. Mass balance relationships of headers are calculated using Equations 18, 19 and 20.
Mass balance relationships of headers

$$\dot{m}_1 = \dot{m}_2 + \dot{m}_3 + \dot{m}_{Letdown,headerHHP} \quad (18)$$

$$\dot{m}_3 + \dot{m}_5 + \dot{m}_{Letdown,headerHHP} = \dot{m}_7 + \dot{m}_8 + \dot{m}_9 + \dot{m}_{10} + \dot{m}_{14} + \dot{m}_{16} + \dot{m}_{18} + \dot{m}_{20} + \dot{m}_{22} + \dot{m}_{24} + \dot{m}_{Letdown,headerHP} \quad (19)$$

$$\dot{m}_{15} + \dot{m}_{17} + \dot{m}_{19} + \dot{m}_{21} + \dot{m}_{23} + \dot{m}_{29} + \dot{m}_{31} + \dot{m}_{36} + \dot{m}_{Letdown,headerHP} = + \dot{m}_{26} + \dot{m}_{38} + \dot{m}_{43} + \dot{m}_{50} + \dot{m}_{51} \quad (20)$$

Results and Discussion

Validation

To validate the results of this study, the operating parameters of two system components under design conditions are compared with the corresponding data obtained from the steam cycle documentation of Petrochemical Unit A, as shown in Table 2.

Cycle Energy, Exergy, and Power Analysis Results

After solving Equations 1-13, the energy and exergy efficiencies and the exergy destruction rate are evaluated for the equipment listed in Table 3 using Engineering Equation Solver (EES) software.

Table 2 Verification of simulation results with the values of design documents of two items of equipment.

Parameter	Design Mode Value	Simulation Mode	Percentage Error
Pump STP-5202	(kW) 2311	(kW) 2460	6.24%
Turbine STC-3002	(kW) 8395	(kW) 8614	2.5%

Table 3 Exergy efficiency and exergy destruction rate of the equipment in the system.

Equipment Name	Energy Efficiency	Exergy Efficiency	Exergy Destruction (kW)
Turbine STC-3002	0.73	0.9416	534.7
Turbine STC-3001	0.7167	0.8119	5800
Turbine CPT-3001	0.3385	0.3831	154.3
Turbine CPT-1001	0.3676	0.4821	138
Turbine STC-1003	0.4732	0.5194	1013
Turbine STC-1002	0.4535	0.5009	598.8
Turbine STP-5202	0.6738	0.6936	1087
Turbine STC-1001	0.6365	0.7582	4798
Pump 5201	0.71	0.6875	501.3
Pump 5202	0.5049	0.824	57.31
Boiler SB-5201		0.825	29509.376
Boiler SB-5202		0.8569	10889.22
Deaerator DA-5201		0.7944	5952
Deaerator DA-5202		0.61	5212
Steam Drum D-5202		0.5846	629.2
Steam Drum D-5203		0.6157	551.7
Condenser STC-3001		0.3354	25286
Condenser STC-1001		0.2752	23313

As seen in Fig. 2, exergy efficiency and exergy destruction rate have been calculated for the equipment available in the steam system. The main boiler (SB-5201), which supplies steam to the HHP header, exhibits the highest exergy destruction rate, whereas the lowest value is observed in pump 5202. The combustion process in the boiler generates significant irreversibilities, resulting in high entropy production and substantial exergy destruction. Exergy destruction represents the loss of useful work potential in a thermodynamic process. As shown in part (b) of the figure, the main steam turbine exhibits the highest second-law efficiency within the cycle. This performance is attributed to the high inlet temperature and pressure of the steam, which enhance the efficiency of energy conversion. Overall, the highest exergy destruction rates are related to boilers and condensers.

The effect of Header Pressure and Temperature on Exergy Efficiency and Net Cycle Power

Based on the obtained values and the graphs in Fig.s 3, 4, and 5, the effects of header temperature and pressure on the cycle's exergy efficiency and net power have been investigated.

The effects of header operating conditions on cycle performance were analyzed. Increasing the temperature of Header 1 reduces exergy efficiency but increases net power output. In contrast, increasing its pressure improves both exergy efficiency and net power. For Header 2, higher temperatures enhance both exergy efficiency and net power, whereas higher pressure has the opposite effect, reducing both parameters. For Header 3, increasing temperature improves both exergy efficiency and net power, while increasing pressure increases exergy efficiency but decreases net power output.

Fig. 3 illustrates the effect of Header 1 operating conditions on system performance. An increase in temperature at Header 1 reduces the exergy efficiency of the system, while enhancing the net power output Conversely, increasing the pressure at Header 1 improves both exergy efficiency and net power.

Fig. 4 shows that increasing the temperature at Header 2 enhances both the system's exergy efficiency and net power output. Conversely, an increase in pressure at Header 2 results in a reduction in both performance indicators.

Fig. 5 shows that increasing the temperature at Header 3 improves both the system's exergy efficiency and net power output. Conversely, an increase in pressure at Header 3 enhances exergy efficiency but reduces net power output.

Solutions to Reduce Water and Energy Consumption in the Intended System

This section presents solutions and scenarios for reducing water and energy consumption in Petrochemical Unit A.

Improving the Steam Consumption of the STC-3001 Condensing Turbine

STC-3001 steam turbine is a condensing turbine with controllable extraction. Steam turbines in petrochemical units typically discharge steam to low-pressure headers; therefore, they are equipped with controllable extraction points to regulate steam extraction. According to the turbine design specifications, the low-pressure (LP) section operates at maximum capacity, whereas the high-pressure (HP) section operates under part-load conditions. From an exergy perspective, steam at higher temperature and pressure is associated with higher specific exergy, which can enhance power output and system efficiency.

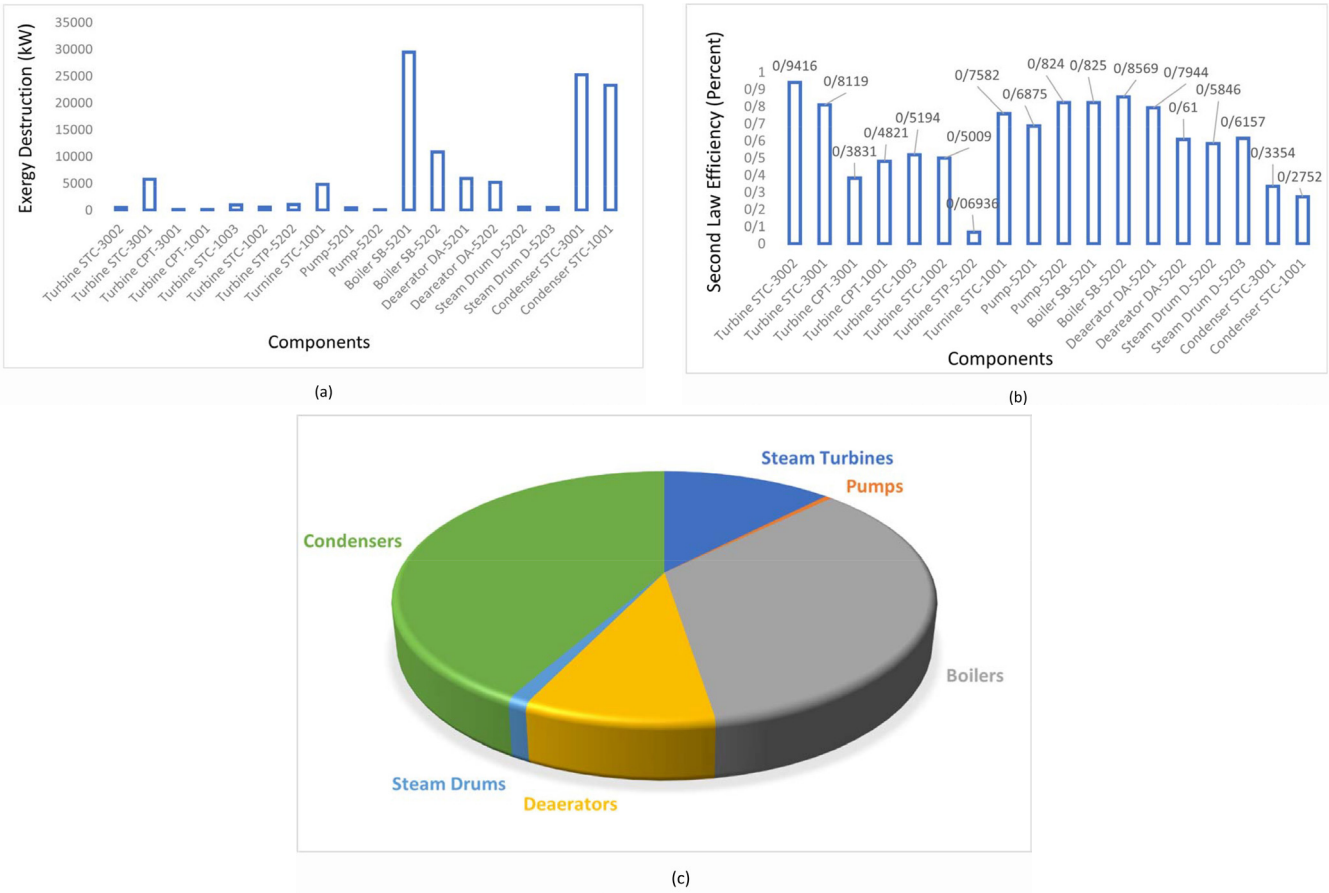

Fig. 2 (a) Contribution of exergy analysis of different components of the steam cycle, (b) Second law efficiency, (c) Exergy destruction per plant's components.

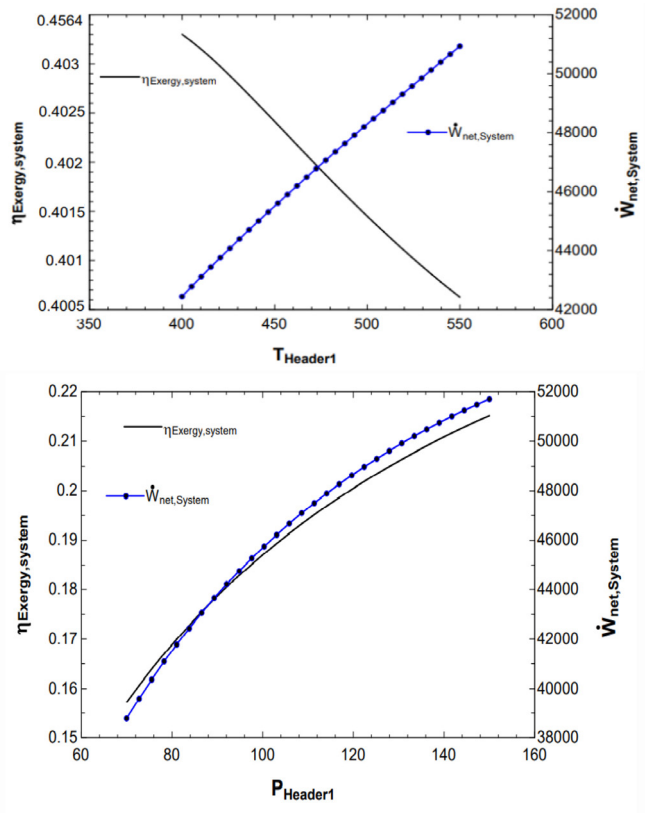

Fig. 3 Changes in exergy efficiency and net cycle power as a function of temperature and pressure of header 1.

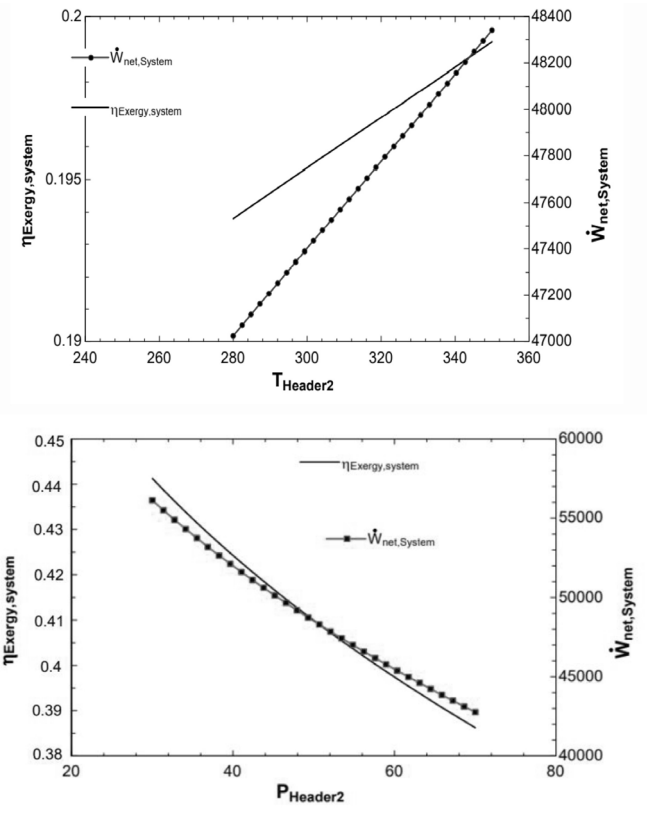

Fig. 4 Changes in exergy efficiency and net cycle power as a function of temperature and pressure of header 2.

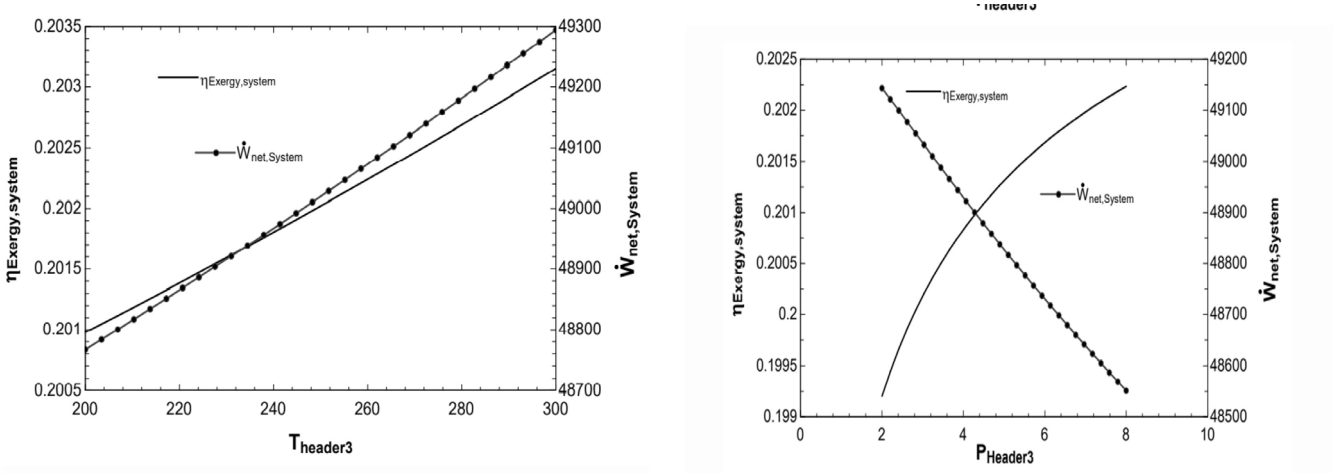

Fig. 5 Changes in exergy efficiency and net cycle power as a function of temperature and pressure of header 3.

Accordingly, increasing the utilization of HHP header steam while reducing HP header steam consumption can improve the overall efficiency of the system. In this section, the Thermoflex module of the Thermoflow software has been employed to observe the intended changes. The operational data of the STC-3001 steam turbine are shown in Fig. 6. Fig. 6 shows that the steam mass flow rate entering the HHP header is 292.6 tons/hour. The mass flow rates to the HP (Point 3) and LP (Point 5) sections of the STC-3001 turbine are 140 and 77.5 tons/hour, respectively. Following the proposed modifications, the HP section flow, supplied via excess steam from the control valve, increased to 162.31 tons/hour under unchanged thermodynamic conditions. In contrast, the steam flow to the LP section and condenser decreased by 64.8 tons/hour, and the steam let-down from the HHP header to the HP header was eliminated. The results are illustrated in Fig. 7. As seen, after applying the intended changes, the amount of steam entering the HHP header at Point 1 has decreased by 10.7 tons/hour. Furthermore, based on the system design-related documents, in the operating conditions of the complex, an amount of 2.11 m^3/h sprayed demin water (deionized water) has been used for desuperheating the steam exiting the let-down between the two HHP and HP steam headers. By applying the intended changes, as well as a decrease in the amount of steam entering the HHP header by 10.7 tons/hour, the amount of 2.11 m^3/h demin water required for desuperheating the steam exiting the valve between the two headers also decreases. Table 4 presents the utility rates used in the economic analysis, whereas Table 5 summarizes the savings achieved after implementing the proposed modifications.

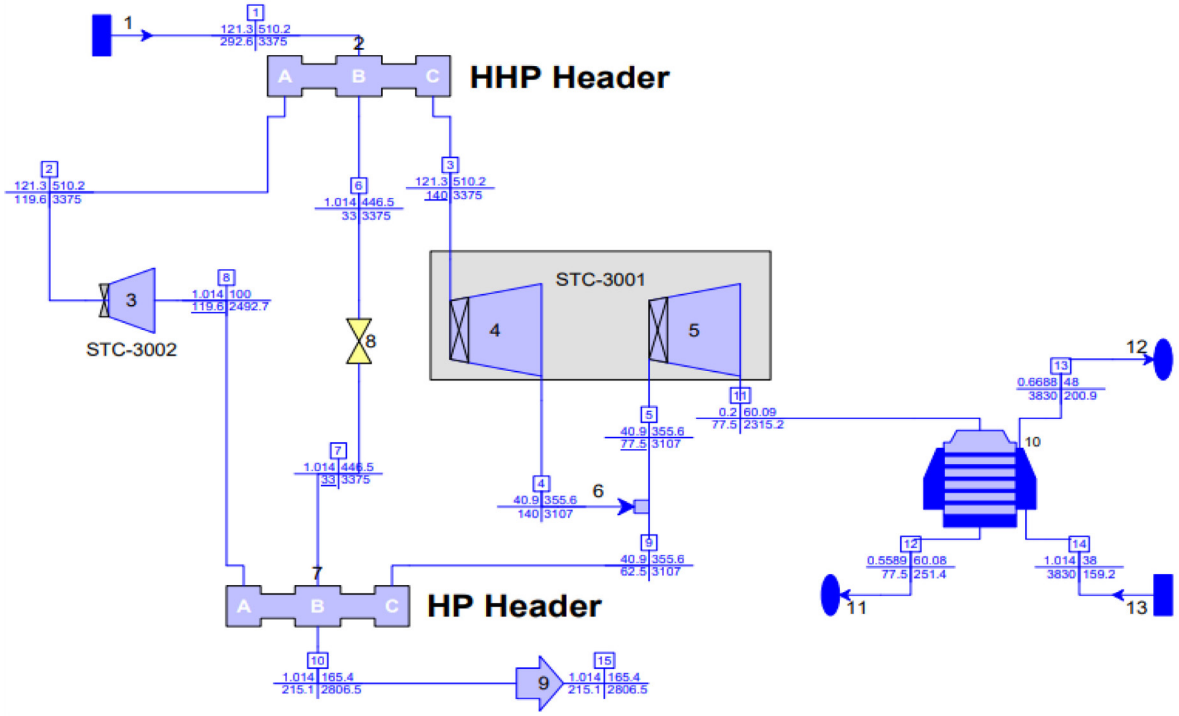

Fig. 6 STC-3001 steam turbine performance data.

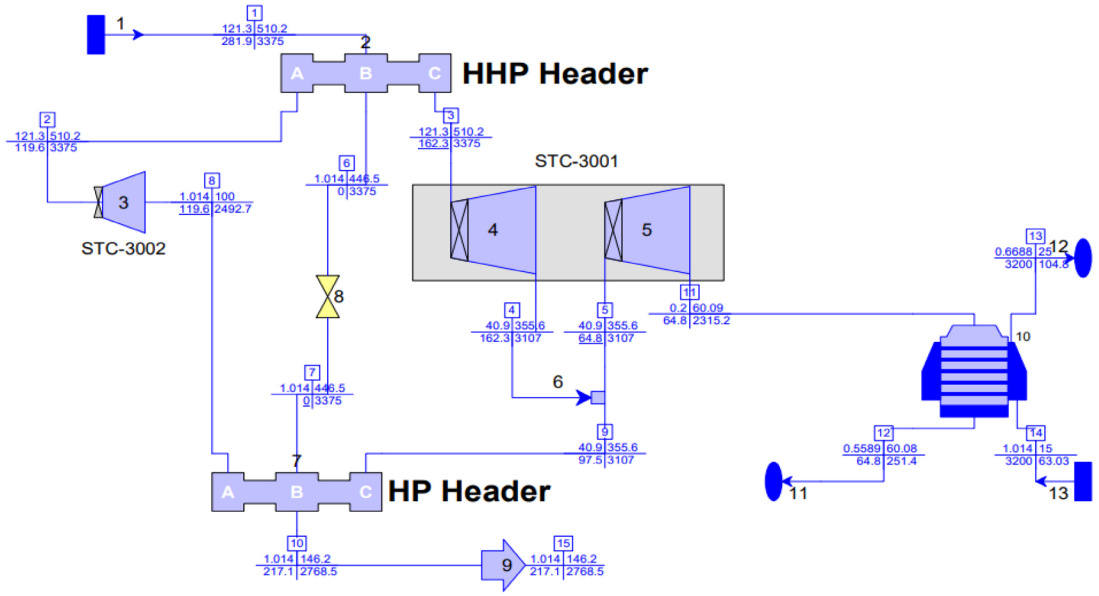

Fig. 7 Simulation results after applying changes in the STC-3001 steam turbine.

Table 4 Utility rates considered for economic calculations [21].

Utility Type	Rate
Steam	15 $/ton
Electricity	0.055 $kWh
Demin Water	1.5 $/m^3
Cooling Water	0.1 $/ton

Table 5 The amount of savings achieved after applying the desired changes.

Steam reduction rate	10.7 ton/hr
The amount of demin water has decreased	2.11 m^3/hr
Savings per hour (in dollars)	163.66 $
Daily savings (in dollars)	3.927.96 $
Annual savings (in dollars)	1.433,705 $

Reducing the Temperature of the Cooling Water Returning from STC-3001 Condenser

Following the implementation of the proposed modifications in the operating conditions of the STC-3001 steam turbine, the steam flow to the HHP header and the demineralized water required for desuperheating the let-down steam between the two headers were reduced. Moreover, the condensate return temperature from the STC-3001 shell-and-tube condenser decreased. Also, the amount of steam has decreased by 4.08%. Fig.s 8 and 9 illustrate the condenser operating conditions before and after the proposed modifications, respectively. In Fig.s 8 and 9, pressure (P) is in bar, temperature (T) is in degrees Celsius, enthalpy (H) is in kJ, an d flow rate (M) is in tons per hour. Also, 'sub' refers to the temperature of the subcooled liquid in degrees Celsius.

Following the implementation of the proposed modifications in the STC-3001 steam turbine, the condensate return temperature decreased by 2.17 °C.

Improving the Pressure Condition of the STC-1001 Steam Turbine Condenser

One of the significant cases in utilizing steam turbines is the proper adjustment of the turbine steam sealing. In condensing turbines, the primary function of steam sealing is to prevent ambient air ingress into the main steam flow, which leads to an increase in non-condensable gases within the condenser and consequently raises the condenser pressure [24].

Table 6 presents the data of the STC-1001 turbine under design and operating conditions.

Table 6 distinguishes between design and operating conditions of the STC-1001 steam turbine, where bold and underlined values indicate the design condition and regular font values indicate the operating condition.

A comparison between the design and operating conditions of the STC-1001 turbine shows that the primary cause of deviation from the design point is the increased condenser pressure. Insufficient sealing steam prevents effective gland sealing, allowing air ingress into the condenser through the gland packings. This increases the concentration of non-condensable gases, raises condenser pressure, and consequently reduces turbine efficiency. As a result, condenser pressure increases from 0.16 to 0.271 bar, leading to an additional HP header steam consumption of 6 tons/hour. After modification of the gland steam system, turbine performance improves and condenser pressure is reduced. Steam consumption is also reduced by 13%. The associated economic savings are presented in Table 7.

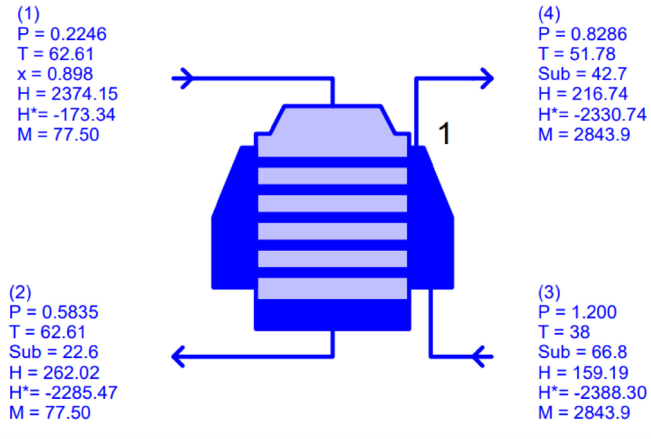

Fig. 8 STC-3001 condenser performance data.

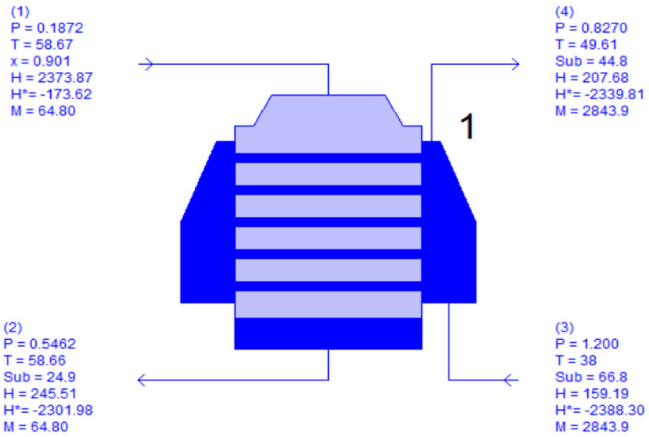

Fig. 9 The results of the STC-3001 condenser data after applying the desired changes to the STC-3001 turbine.

Table 6 STC-1001 steam turbine design and operational mode data [21].

Features	Mass Flow Rate (ton/hr)		Pressure (bar)		Temperature (°C)	
Inlet to turbine from HHP header	40.45	46.5	42.4	40.9	375	375.81
Inlet to turbinefrom LP header	52.95	45.29	4.4	4.8	218	214.3108
Output from the turbine and input to the condenser	93.4	91.79	0.16	0.271	53	53

Table 7 Savings from STC-1001 Steam Turbine Gland System Improvements.

The amount of steam consumption reduction of the HP header	6 t/h
Savings per hour (in dollars)	90 $/h
Daily savings (in dollars)	2160 $
Annual savings (in dollars)	788,400 $

Conclusions

In this article, the water-energy nexus is investigated in the third phase of urea and ammonia of Petrochemical Company A. The system is divided into 51 state points, and the temperature, pressure, and mass flow rate at each point are used as input data. The governing energy and exergy equations, together with mass balance relations, are solved using Engineering Equation Solver (EES). Furthermore, the Thermoflex module of ThermoFlow software is employed for additional simulation and system analysis. The following section presents the results and proposed solutions for reducing steam and energy consumption According to the STC-3001 steam turbine design documents, the LP section operates at maximum capacity, whereas the HP section operates well below its design condition. Following the implementation of the proposed modifications, the steam flow to the HHP header at Point 1 decreased to 10.7 tons/hour. Moreover, the demineralized water consumption for desuperheating the steam from the inter-header valve was reduced by 2.11 m³/h, resulting in annual savings of $1,433,705.

- Considering applying the intended changes to the operational data of the STC-3001 steam turbine, The outlet temperature of the STC-3001 shell-and-tube condenser decreased by 2.17 °C.
- Ultimately, comparing the data of the STC-1001 turbine design and operating states has indicated that the main reason for the deviation from the design state conditions is the condenser's increased pressure. An increase in condenser pressure from 0.16 to 0.271 bar resulted in air ingress through the gland packings, leading to a higher concentration of non-condensable gases and, consequently, a reduction in turbine efficiency. Thus, by proper adjustment of the steam sealing, culminating in saving approximately 6 tons/hour of steam consumption, which is equivalent to an annual savings of $778,400.

Acknowledgments

I would like to express my sincere gratitude to the Research Institute of Petroleum Industry (RIPI) for their unwavering support and provision of resources throughout the course of this research. The research facilities and infrastructure provided by the Research Institute of Petroleum Industry (RIPI) have played a significant role in the successful completion of this study.

Conflict of Interest and Funding

No funds are used in this research and manuscript.

Nomenclature

Abbreviations

HHP: High High Pressure
HP: High Pressure
LP: Low Pressure
LHV: Low Heating Value
ST:Steam Turbine

Latin Symbols

$\dot{m}$: Mass Flow Rate (t/h)
$\dot{m}_f$: Fuel Mass Flow Rate (t/h)
P: Pressure (bar)

T: Temperature (°C)
I: Exergy Destruction (kW)
Ex: Exergy
H: Enthalpy (kJ)
S: Entropy (J/K)
W: Work (kJ)

Greek Symbols
Ψ: Physical Exergy
η_{th}: Thermal Efficiency
η_{exergy}: Exergy Efficiency
γ_f:Exergy Factor

Subscripts
a: Actual
s: Isentropic
i: Inlet
o: utlet
P: Pump
T: Turbine
F: Fuel

References

1. Pan, S. Y., Snyder, S. W., Packman, A. I., Lin, Y. J., & Chiang, P. C. (2018). Cooling water use in thermoelectric power generation and its associated challenges for addressing water-energy nexus. Water-Energy Nexus, 1(1), 26-41. doi: 10.1016/j.wen.2018.04.002.
2. Dai, J., Wu, S., Han, G., Weinberg, J., Xie, X., Wu, X., Song, X., Jia, B., Xue, W. and Yang, Q., (2018). Water-energy nexus: A review of methods and tools for macro-assessment. Applied Energy, 210, 393-408. doi.org/10.1016/j.apenergy.2017.08.243.
3. Gorjian, S., & Ghobadian, B. (2015). Solar desalination: A sustainable solution to water crisis in Iran. Renewable and Sustainable Energy Reviews, 48, 571-584. doi: 10.1016/j.rser.2015.04.009.
4. Biancalani, R., & Marinelli, M. (2021). Assessing SDG indicator 6.4. 2 'level of water stress' at major basins level. UCL Open Environment, 3, e026. doi: 10.14324/111.444/ucloe.000026.
5. Altarawneh, O. R., Alsarayreh, A. A., Ala'a, M., Al-Kheetan, M. J., & Alrwashdeh, S. S. (2022). Energy and exergy analyses for a combined cycle power plant in Jordan. Case Studies in Thermal Engineering, 31, 101852. doi: 10.1016/j.csite.2022.101852.
6. Hamayun, M. H., Hussain, M., Shafiq, I., Ahmed, A., & Park, Y. K. (2022). Investigation of the thermodynamic performance of an existing steam power plant via energy and exergy analyses to restrain the environmental repercussions: A simulation study. Environmental Engineering Research, 27(1). doi: 10.4491/eer.2020.683.
7. Gungor Celik, A., & Aydemir, U. (2025). Energy, exergy analysis and sustainability assessment of a thermal power plant operating in various environmental conditions using real operational data. Sustainability, 17(4), 1417. doi.org/10.3390/su17041417.
8. Tontu, M., Sahin, B., & Bilgili, M. (2024). Using energy and exergy analysis to compare different coal-fired power plants. Energy Sources, Part A: Recovery, Utilization, and Environmental Effects, 46(1), 4314-4329. doi: 10.1080/15567036.2019.1696429.
9. Mohseni, M., Bahrami, H. R., & Leili, M. S. (2024). Energy and exergy analysis of a steam power plant to replace the boiler with a heat recovery steam generator. International Journal of Exergy, 43(1), 1-20. doi: 10.1504/IJEX.2024.136448.
10. Azubuike, U. G., Egbuhuzor, L. C., Njoku, H. O., & Ekechukwu, O. V. (2023). Exergy analysis of a steam power plant at full and partial load conditions. International Journal of Exergy, 40(2), 182-197. doi: 10.1504/ijex.2023.128784.
11. Galal, M., Abd El-Maksoud, R., & Bayomi, N. N. (2024). Exergy analysis of a steam power station in a sulfuric acid plant. Case Studies in Thermal Engineering, 53, 103937. doi: 10.1016/j.csite.2023.103937.
12. Walker, M. E., Lv, Z., & Masanet, E. (2013). Industrial steam systems and the energy-water nexus. Environmental science & technology, 47(22), 13060-13067. doi: 10.1021/es403715z.
13. Hu, H., Li, Z., Jiang, Y., & Du, X. (2018). Thermodynamic characteristics of thermal power plant with hybrid (dry/wet) cooling system. Energy, 147, 729-741. doi: 10.1016/j.energy.2018.01.074.
14. Asvapoositkul, W., & Kuansathan, M. (2014). Comparative evaluation of hybrid (dry/wet) cooling tower performance. Applied Thermal Engineering, 71(1), 83-93. doi: 10.1016/j.applthermaleng.2014.06.023.
15. Ahmadi, G., Toghraie, D., & Akbari, O. (2019). Energy, exergy and environmental (3E) analysis of the existing CHP system in a petrochemical plant. Renewable and Sustainable Energy Reviews, 99, 234-242. doi: 10.1016/j.rser.2018.10.009.
16. Ahmadi, G. R., & Toghraie, D. (2016). Energy and exergy analysis of Montazeri steam power plant in Iran. Renewable and Sustainable Energy Reviews, 56, 454-463. doi: 10.1016/j.rser.2015.11.074.
17. Ali, B. (2018). Forecasting model for water-energy nexus in Alberta, Canada. Water-Energy Nexus, 1(2), 104-115. doi: 10.1016/j.wen.2018.08.002.
18. Vandani, A. M. K., Bidi, M., & Ahmadi, F. (2015). Exergy analysis and evolutionary optimization of boiler blowdown heat recovery in steam power plants. Energy Conversion and Management, 106, 1-9. doi: 10.1016/j.enconman.2015.09.018.
19. Gu, A., Teng, F., & Wang, Y. (2014). China energy-water nexus: Assessing the water-saving synergy effects of energy-saving policies during the eleventh Five-year Plan. Energy Conversion and Management, 85, 630-637. doi: 10.1016/j.enconman.2014.04.054.
20. Khaleel, O. J., Ismail, F. B., Ibrahim, T. K., & bin Abu Hassan, S. H. (2022). Energy and exergy analysis of the steam power plants: A comprehensive review on the Classification, Development, Improvements, and configurations. Ain Shams Engineering Journal, 13(3), 101640. doi: 10.1016/j.asej.2021.11.009.
21. Shahidian, A., Davoudian, M., & Habibi, M. R. (2024) Providing the Best Energy-Exergy-Water Nexus Based Strategy for a Petrochemical Unit. Available at SSRN, 5039142-5039168.
22. I. Dincer and M. A. Rosen, Energy, Environment and Sustainable Development, Second edition, Ontario,

Elsevier, 2013, 1-537.
23. Y. A. , Boles, Michael A., Kanoglu, Mehmet THERMODYNAMICS 9th edition, vol. 44, no. 8. 2019.
24. Leyzerovich, A. S. (2021). Steam turbines for modern fossil-fuel power plants. River Publishers.